

CHAPTER THIRTY TWO

METHOD FOR ESTIMATING DIRECTIONAL WAVE SPECTRUM IN INCIDENT AND REFLECTED WAVE FIELD

by

Masahiko Isobe* and Kosuke Kondo**

ABSTRACT

The relationship between the directional spectrum and the cross-power spectra in an incident and reflected wave field differs from the situation with no reflected waves because the phase lag between the incident and reflected waves is not random. Extra terms, which may be called phase interaction terms, exist. Hence standard methods for estimating the directional spectrum are not applicable. In the present study, the MLM is modified for this situation and the method is termed the MMLM (Modified Maximum Likelihood Method).

The validity of the MMLM is examined by numerical simulation. The results indicate that the MMLM has a high resolution power. Formulas to determine the reflection coefficient are derived and their accuracy and suitability are examined.

1. INTRODUCTION

This paper describes a method to measure the directional spectrum in an incident and reflected wave field and to determine the reflection coefficient of a structure in a directional sea. The directional spectrum represents the energy distribution in wave direction, so that in principle the incident and reflected wave energies can be separated by measuring the directional spectrum near a structure and then the reflection coefficient can be determined. However, standard methods of estimating the directional spectrum are not valid because the phase lag between the incident and reflected waves is not random. Therefore, these methods should be modified for application in such a situation.

Many methods have been proposed for directional spectrum estimation. These are the DFT method (Direct Fourier Transform Method; Barber, 1963), parametric methods (Longuet-Higgins et al., 1963; Panicker and Borgman, 1974), the MLM (Maximum Likelihood Method; Capon,

* Associate Professor, Department of Civil Engineering, Yokohama National University, 156 Tokiwadai, Hodogaya-ku, Yokohama, 240 Japan

** Principal Engineer, Design and Engineering Department, Penta-Ocean Construction Co., Ltd., 2-2-8 Koraku, Bunkyo-ku, Tokyo, 112 Japan

1969), and others. Of all the proposed methods of calculation, the MLM has the highest resolution power, so that it is favorable to use to separate the incident and reflected wave energies. Therefore, in the present study, the MLM is modified to estimate the directional spectrum in an incident and reflected wave field.

Numerical simulations were carried out to examine the validity of the MMLM. By this means, accuracies of various formulas to determine the reflection coefficient could be examined.

The MLM was originally applicable only to wave gage arrays, but recently it has been extended for use with mixed gage arrays such as a pitch-roll buoy system, a clover-leaf buoy system, a wave gage plus current meter system, and so on (Isobe et al., 1984; Oltman-Shay and Guza, 1984). Hence it is also possible to extend the present method to mixed measuring systems.

2. DERIVATION OF MMLM

2.1 Relationship between Directional Spectrum and Cross-Power Spectra

Suppose that the wave amplitude is small, and that the water surface elevation can be expressed as the superposition of component waves with wavenumber (vector), \mathbf{k} , and angular frequency, σ . The water surface elevation due to the incident waves, η_i , at the point, \mathbf{x} , and the time, t , can be expressed as:

$$\eta_i(\mathbf{x}, t) = \int_{\sigma} \int_{\mathbf{k}} e^{i(\mathbf{k}\mathbf{x} - \sigma t)} Z(d\mathbf{k}, d\sigma) \quad (1)$$

This was called the spectral representation by Koopmans (1974). From the physical point of view, $Z(d\mathbf{k}, d\sigma)$ means the amplitude which represents the energy within $[\mathbf{k}, \mathbf{k} + d\mathbf{k}]$ and $[\sigma, \sigma + d\sigma]$. The quantity Z is a complex number. The absolute value of Z gives the amplitude of the component waves and the argument gives the phase at $\mathbf{x} = \mathbf{0}$ and $t = 0$. Since the phase lag between different wave components can be assumed to be random, $Z(d\mathbf{k}, d\sigma)$ and $Z(d\mathbf{k}', d\sigma')$ are independent for $\mathbf{k} \neq \mathbf{k}'$, i.e.,

$$\langle Z(d\mathbf{k}, d\sigma) Z^*(d\mathbf{k}', d\sigma') \rangle = 0 \quad (\mathbf{k} \neq \mathbf{k}') \quad (2)$$

where the symbol $\langle \rangle$ denotes the ensemble mean. The wavenumber-frequency spectrum, $S(\mathbf{k}, \sigma)$, represents the power density (square of the amplitude), and is therefore defined as:

$$\langle Z(d\mathbf{k}, d\sigma) Z^*(d\mathbf{k}, d\sigma) \rangle = S(\mathbf{k}, \sigma) d\mathbf{k} d\sigma \quad (3)$$

where the symbol $*$ denotes the complex conjugate. The wavenumber vector, \mathbf{k} , is expressed by the wavenumber, k , and the wave propagation direction, θ . Hence, the wavenumber-frequency spectrum is a function of k , θ , and σ . For water surface waves, since k is uniquely determined from σ by the dispersion relation, the spectrum becomes a function of θ and σ and is called directional spectrum.

As shown in Fig. 1, if waves are reflected at the y-axis, the water surface elevation due to the reflected waves, η_r , can be expressed as:

$$\eta_r(\mathbf{x}, t) = \int_{\sigma} \int_{\mathbf{k}} r e^{i(\mathbf{k}_r \mathbf{x} - \sigma t)} Z(d\mathbf{k}, d\sigma) \tag{4}$$

where \mathbf{k}_r denotes the vector symmetrical to \mathbf{k} with respect to the reflection line, and r is the reflection coefficient which can be a function of \mathbf{k} and/or σ . Even though the amplitude of the reflected waves may change by the factor r , the phase on the reflection line is the same as that of the corresponding incident waves. Therefore the phase lag between the incident and reflected waves is not random. Let \mathbf{x}_r be the vector symmetrical to \mathbf{x} , then Eq. (4) can be written as:

$$\eta_r(\mathbf{x}, t) = \int_{\sigma} \int_{\mathbf{k}} r e^{i(\mathbf{k} \mathbf{x}_r - \sigma t)} Z(d\mathbf{k}, d\sigma) \tag{5}$$

From Eqs. (1) and (5), the total water surface elevation, $\eta = \eta_i + \eta_r$, can be expressed as:

$$\eta(\mathbf{x}, t) = \int_{\sigma} \int_{\mathbf{k}} [e^{i(\mathbf{k} \mathbf{x} - \sigma t)} + r e^{i(\mathbf{k} \mathbf{x}_r - \sigma t)}] Z(d\mathbf{k}, d\sigma) \tag{6}$$

Thus the complex amplitude, $X(\mathbf{x}, d\sigma)$, which represents the energy in $[\sigma, \sigma + d\sigma]$ at the point \mathbf{x} , becomes

$$X(\mathbf{x}, d\sigma) = \int_{\mathbf{k}} [e^{-i\mathbf{k} \mathbf{x}} + r e^{-i\mathbf{k} \mathbf{x}_r}] Z^*(d\mathbf{k}, d\sigma) \tag{7}$$

The cross-power spectrum, $\Phi_{mn}(\sigma)$, between the water surface elevations at $\mathbf{x} = \mathbf{x}_m$ and $\mathbf{x} = \mathbf{x}_n$ is defined as the ensemble mean of the product of the complex amplitude, $X(\mathbf{x}_m, d\sigma)$, the the complex conjugate amplitude, $X^*(\mathbf{x}_n, d\sigma)$. That is ,

$$\Phi_{mn}(\sigma) d\sigma = \langle X^*(\mathbf{x}_n, d\sigma) X(\mathbf{x}_m, d\sigma) \rangle \tag{8}$$

If $m = n$, then $\Phi_{mn}(\sigma)$ represents the power spectrum, and if $m \neq n$, $\Phi_{mn}(\sigma)$ represents the cross spectrum. Substitution of Eq. (7) into Eq. (8) yields

$$\begin{aligned} \Phi_{mn}(\sigma) d\sigma = \int_{\mathbf{k}} \int_{\mathbf{k}'} [e^{i\mathbf{k} \mathbf{x}_m + r e^{i\mathbf{k} \mathbf{x}_m} }] [e^{-i\mathbf{k}' \mathbf{x}_n + r e^{-i\mathbf{k}' \mathbf{x}_n} }] \\ \times \langle Z(d\mathbf{k}, d\sigma) Z^*(d\mathbf{k}', d\sigma) \rangle \end{aligned} \tag{9}$$

From Eqs. (2) and (3), Eq. (9) becomes

$$\Phi_{mn}(\sigma) = \int_{\mathbf{k}} [e^{i\mathbf{k} \mathbf{x}_m + r e^{i\mathbf{k} \mathbf{x}_m} }] [e^{-i\mathbf{k} \mathbf{x}_n + r e^{-i\mathbf{k} \mathbf{x}_n} }] S(\mathbf{k}, \sigma) d\mathbf{k} \tag{10}$$

This is the relationship between the wavenumber-frequency (or directional) spectrum and the cross-power spectrum in an incident and reflected wave field and will be used to derive the basic formula for

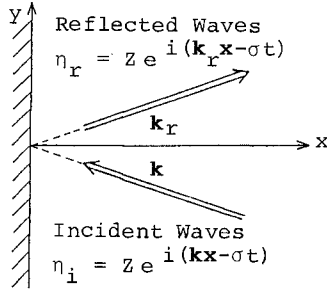


Fig. 1 Definition sketch of incident and reflected wave field.

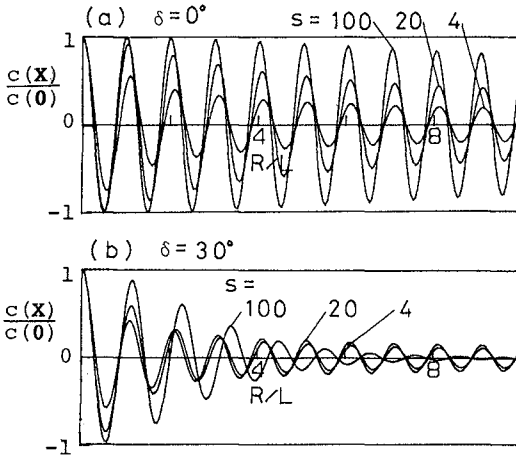


Fig. 2 Co-spectrum for Mitsuyasu-type directional distribution functions.

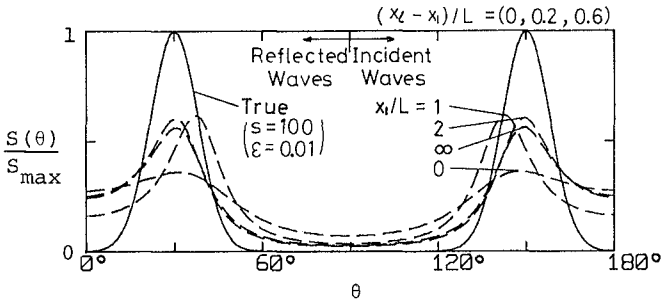


Fig. 3 Result of directional spectrum estimation by the standard MLM in incident and reflected wave field.

estimating the directional spectrum. The product of the first terms in the two brackets in Eq. (10) represents the incident wave component and the product of the second terms represents the reflected wave component. The other two products are extra terms describing the interaction of the incident and reflected wave fields. Since these terms appear because the phase lag between the incident and reflected waves is not random, they may be called phase interaction terms.

2.2 Magnitude of Phase Interaction Contribution

Before proceeding to the discussion of the directional spectrum estimation, it is worth examining the relative magnitude of the phase interaction terms. Any combination of terms in the brackets in Eq. (10) has the following form:

$$\phi(\mathbf{X}) = \int_{\mathbf{k}} e^{-i\mathbf{k}\mathbf{X}} S(\mathbf{k}, \sigma) d\mathbf{k} \quad (11)$$

Mitsuyasu et al. (1974) proposed a standard directional distribution function with two parameters, θ_0 and s , as:

$$S(\mathbf{k}, \sigma) = \left[\cos \frac{\theta - \theta_0}{2} \right]^{2s} \quad (12)$$

If Eq. (12) is substituted into Eq. (11), the following result can be obtained after some manipulation:

$$\frac{c(\mathbf{X})}{c(\mathbf{0})} = J_0(kR) + 2 \sum_{l=1}^{[[s/2]]} (-1)^l \left[\frac{s!}{(s-2l)!} \right] \left[\frac{s!}{(s+2l)!} \right] \times J_{2l}(kR) \cos\{2l(\theta_0 - \theta)\} \quad (13)$$

$$\frac{q(\mathbf{X})}{c(\mathbf{0})} = 2 \sum_{l=0}^{[(s-1)/2]} (-1)^l \left[\frac{s!}{(s-2l-1)!} \right] \left[\frac{s!}{(s+2l+1)!} \right] \times J_{2l+1}(kR) \cos\{(2l+1)(\theta_0 - \theta)\} \quad (14)$$

where $[[x]]$ denotes the maximum integer not larger than x , J_n is a Bessel function of the n 'th order, and c and q are the co- and quadrature-spectra:

$$\phi(\mathbf{X}) = c(\mathbf{X}) - iq(\mathbf{X}) \quad (15)$$

and

$$\mathbf{X} = (R \cos \theta, R \sin \theta) \quad (16)$$

Figure 2 shows the relative co-spectrum as a function of relative distance R/L (L : wave length) for $\delta = \theta_0 - \theta = 0^\circ$ and 30° . For the quadrature-spectrum, the shapes of the curves are similar to the co-spectrum, but the maximum and minimum occur at the zero-crossing points of the co-spectrum. Thus the amplitude of ϕ becomes the envelope of the curve. Therefore, the relative magnitude of ϕ is small for large

relative distance, unless the directional distribution is very narrow (s is large) and the principal direction almost coincides with the direction of the distance vector ($\theta = \theta_0$).

For the phase interaction terms, we have $\mathbf{X} = \mathbf{x}_{nr} - \mathbf{x}_m$, $\mathbf{x}_n - \mathbf{x}_{mr}$, so that R becomes about twice the distance between the measuring point and the reflection line. Hence the phase interaction terms generally become small if the wave gage array is located far from the reflection line. Therefore, if the structure is long enough, the incident and reflected directional spectrum can be observed in the far field by applying the standard methods of estimation.

Figure 3 is an example of a numerical simulation which shows the effect of the phase interaction terms. The peak incident wave direction is 150° and the reflection coefficient is 1, so that a spectral peak due to reflected waves appears at $\theta = 30^\circ$. The separation distance in the 3-sensor linear wave gage array are $0.2L$ and $0.4L$. The estimated directional spectra by the standard MLM are shown by the dashed lines for the cases that the distances between the nearest wave gage and the reflection line are 0 , L , $2L$, and ∞ . The accuracy becomes higher as the distance increases. This is because the phase interaction terms become small. However, a 3-sensor array may not be sufficient to measure a bimodal directional spectrum.

2.3 Formula for Estimating the Directional Spectrum

In this subsection a formula for estimating the directional spectrum is derived from the relationship between the directional spectrum and the cross-power spectra, as given by Eq. (10). The maximum likelihood technique is used and the process is similar to that given by Davis and Regier (1977), and Isobe et al. (1984).

Let

$$\gamma_{on}(\mathbf{k}) = e^{-i\mathbf{k}\cdot\mathbf{x}_{om}} + r e^{-i\mathbf{k}\cdot\mathbf{x}_{mr}} \quad (17)$$

and

$$T_{mn}(\mathbf{k}) = \gamma_{on}^*(\mathbf{k}) \gamma_{on}(\mathbf{k}) \quad (18)$$

Then Eq. (10) can be rewritten as follows:

$$\phi_{mn}(\sigma) = \int_{\mathbf{k}'} T_{mn}(\mathbf{k}') S(\mathbf{k}', \sigma) d\mathbf{k}' \quad (19)$$

In general, the estimated wavenumber-frequency spectrum, denoted with a caret as $\hat{S}(\mathbf{k}, \sigma)$, can be formally expressed as a linear combination of the known cross-power spectra:

$$\hat{S}(\mathbf{k}, \sigma) = \sum_m \sum_n \alpha_{mn}(\mathbf{k}) \phi_{mn}(\sigma) \quad (20)$$

where Σ means a summation over all measuring points and the $\alpha_{mn}(\mathbf{k})$ are coefficients. Then, substitution of Eq. (19) into Eq. (20) yields

$$\hat{S}(\mathbf{k}, \sigma) = \int_{\mathbf{k}'} S(\mathbf{k}', \sigma) w(\mathbf{k}, \mathbf{k}') d\mathbf{k}' \tag{21}$$

where

$$w(\mathbf{k}, \mathbf{k}') = \sum_m \sum_n \alpha_{mn}(\mathbf{k}) T_{mn}(\mathbf{k}') \tag{22}$$

Equation (21) indicates that the estimated wavenumber-frequency spectrum is a convolution of the true wavenumber-frequency spectrum and the window function, $w(\mathbf{k}, \mathbf{k}')$, which is expressed by Eq. (22).

Now α_{mn} is assumed to be of factorable form as

$$\alpha_{mn}(\mathbf{k}) = \gamma_m(\mathbf{k}) \gamma_n^*(\mathbf{k}) \tag{23}$$

Then Eqs. (20) and (22) become

$$\hat{S}(\mathbf{k}, \sigma) = \sum_m \sum_n \gamma_m(\mathbf{k}) \phi_{mn}(\sigma) \gamma_n^*(\mathbf{k}) \tag{24}$$

and

$$w(\mathbf{k}, \mathbf{k}') = \sum_m \sum_n \gamma_m(\mathbf{k}) T_{mn}(\mathbf{k}') \gamma_n^*(\mathbf{k}) \tag{25}$$

Substitution of Eq. (18) into (25) yields

$$w(\mathbf{k}, \mathbf{k}') = \left| \sum_m \gamma_m(\mathbf{k}) \gamma_{\text{cm}}^*(\mathbf{k}') \right|^2 \tag{26}$$

which shows the value of the window function is non-negative. Then the estimated directional spectrum is always non-negative because the integrand in Eq. (21) is non-negative.

The window function is normalized by putting

$$w(\mathbf{k}, \mathbf{k}) = 1 \tag{27}$$

In order for $\hat{S}(\mathbf{k}, \sigma)$ to closely approximate $S(\mathbf{k}, \sigma)$, it is seen from Eq. (21) that $w(\mathbf{k}, \mathbf{k}')$ should approach the Dirac delta function as closely as possible. Since $S(\mathbf{k}, \sigma)$ and $w(\mathbf{k}, \mathbf{k}')$ in Eq. (21) are non-negative, this can be attained by minimizing the value of $\hat{S}(\mathbf{k}, \sigma)$:

$$\hat{S}(\mathbf{k}, \sigma) \rightarrow \min. \tag{28}$$

From Eqs. (24), (25), (27), and (28), this problem becomes as follows:

$$\frac{\sum_m \sum_n \gamma_m(\mathbf{k}) T_{mn}(\mathbf{k}) \gamma_n^*(\mathbf{k})}{\sum_m \sum_n \gamma_m(\mathbf{k}) \phi_{mn}(\sigma) \gamma_n^*(\mathbf{k})} \rightarrow \max. \tag{29}$$

This is equivalent to the problem of finding the maximum eigenvalue for given matrices, ϕ_{mn} and T_{mn} such that

$$\sum_n T_{mn} \gamma_n^* = \lambda \sum_n \phi_{mn} \gamma_n^* \tag{30}$$

and hence

$$\sum_m \sum_n \phi_{lm}^{-1} T_{mn} \gamma_n^* = \lambda \gamma_l^* \tag{31}$$

where ϕ_{lm}^{-1} is the inverse matrix of ϕ_{lm} . From Eq. (29), the maximum eigenvalue, λ_{max} , is inversely proportional to the estimated directional spectrum:

$$\hat{S}(k, \sigma) \propto 1/\lambda_{max} \tag{32}$$

It can be seen from Eq. (18) that any vector orthogonal to γ_{0n} is an eigenvector with eigenvalue $\lambda = 0$ in Eq. (31). Hence the only possible choice of γ_n for a positive eigenvalue is of the form

$$\gamma_n = \gamma_{0n} + \gamma_{0n}^\perp \tag{33}$$

where γ_{0n}^\perp is a vector orthogonal to γ_{0n} . If Eqs. (18) and (33) are substituted into Eq. (31) and then multiplied with γ_{0l} from the left, the maximum eigenvalue, λ_{max} , can be obtained as

$$\lambda_{max} = \sum_m \sum_n \gamma_{0m} \phi_{mn}^{-1} \gamma_{0n}^* \tag{34}$$

As seen from Eq. (17), λ_{max} is a function of r . In order to determine the value of r , a relationship which is strictly satisfied in the uni-directional case was derived. That is

$$d\lambda_{max} / dr = 0 \tag{35}$$

This relationship is assumed to be valid in a general case and then substitution of Eq. (17) and (34) into Eq. (35) yields

$$r_0 = - \frac{\sum_m \sum_n \phi_{mn}^{-1}(\sigma) [e^{ik(x_n - x_{nr})} + e^{ik(x_{nr} - x_n)}]}{2 \sum_m \sum_n \phi_{mn}^{-1}(\sigma) e^{ik(x_{nr} - x_{nr})}} \tag{36}$$

Since the value of the reflection coefficient is non-negative the estimated reflection coefficient becomes

$$\hat{r} = \begin{cases} 0 & (r_0 \leq 0) \\ r_0 & (r_0 > 0) \end{cases} \tag{37}$$

Finally, from Eqs. (17), (32), (34), and (37), the estimated directional spectrum becomes as follows:

$$\hat{S}(\mathbf{k}, \sigma) = \begin{cases} \kappa / \left[\sum_m \sum_n \Phi_{mn}^{-1}(\sigma) e^{i\mathbf{k}(\mathbf{x}_n - \mathbf{x}_m)} \right] & (r_0 \leq 0) \\ \kappa / \left[\sum_m \sum_n \Phi_{mn}^{-1}(\sigma) e^{i\mathbf{k}(\mathbf{x}_n - \mathbf{x}_m)} \right. \\ \left. - \frac{\left\{ \sum_m \sum_n \Phi_{mn}^{-1}(\sigma) \left[e^{i\mathbf{k}(\mathbf{x}_n - \mathbf{x}_{nr})} + e^{i\mathbf{k}(\mathbf{x}_{nr} - \mathbf{x}_m)} \right] \right\}^2}{4 \sum_m \sum_n \Phi_{mn}^{-1}(\sigma) e^{i\mathbf{k}(\mathbf{x}_{nr} - \mathbf{x}_{mr})}} \right] & (r_0 > 0) \end{cases} \quad (38)$$

where κ is a proportionality constant which can be determined from the relationship between the directional spectrum and the power spectrum. This relationship can be obtained by putting $m = n$ in Eq. (10). The result is

$$\Phi_{mn}(\sigma) = \int_{\mathbf{k}_i} \left[\hat{S}(\mathbf{k}_i, \sigma) + 2 \sqrt{\hat{S}(\mathbf{k}_i, \sigma) \hat{S}(\mathbf{k}_r, \sigma)} \cos \mathbf{k}_i(\mathbf{x}_m - \mathbf{x}_{nr}) + \hat{S}(\mathbf{k}_r, \sigma) \right] d\mathbf{k}_i \quad (39)$$

where \mathbf{k}_i represents the wavenumber vector within the incident wave direction and \mathbf{k}_r is the reflected wavenumber vector corresponding to \mathbf{k}_i . The symbol $\hat{S}(\mathbf{k}_r, \sigma) = r^2 \hat{S}(\mathbf{k}_i, \sigma)$ represents the reflected wave spectrum. If Eq. (38) is substituted into Eq. (39), the equation for determining the value of κ can be obtained for each measuring point. Hence κ can be obtained by the least square method.

Equation (38) was derived by modifying the standard MLM for use in an incident and reflected wave field. Therefore, the present method is named the MMLM (Modified Maximum Likelihood Method).

The procedure for calculating the directional spectrum by the MMLM is summarized as follows:

- 1) For a given data set, compute the cross-power spectra, $\Phi_{mn}(\sigma)$, for all possible combinations.
- 2) For a fixed value of σ , determine k from the dispersion relation and then compute the directional spectrum by using Eq. (38), except for κ . The computation range of the wave direction includes both the incident and reflected wave directions.
- 3) Determine the value of κ from Eq. (39); then the directional spectrum is completely determined by Eq. (38).

3. NUMERICAL SIMULATION

3.1 Procedure of Numerical Simulations

Numerical simulations were performed to examine the validity of the MMLM. The procedure is similar to the one used for examining the EMLM (Isobe et al., 1984). Since from the theoretical viewpoint the energies distributed among the wave frequency can be separated by cross-power spectral analysis, the directional spectrum is described as a function of only the wave direction, θ .

The procedure for the numerical simulation is as follows:

- 1) Specify a functional form for the directional spectrum, $S_{\theta}(\theta)$, and reflection coefficient, $r(\theta)$. Here, the Mitsuyasu-type directional distribution expressed by Eq. (12) is used. To fabricate a bimodal distribution, two Mitsuyasu-type distribution functions with different θ_0 and s are superimposed.
- 2) Calculate ϕ_{mn} for a given wave gage array from Eq. (10). For the power spectra, ϕ_{mm} , a fraction of the total incident wave energy is added as a noise component.
- 3) Calculate $\hat{S}_{\theta}(\theta)$ from Eq. (38) and compare to $S_{\theta}(\theta)$.

3.2 Results

Figure 4 shows an example of the numerical simulation. A 3-sensor linear wave gage array in which the gages are set at $(x, y) = (0.2L, 0)$, $(0.4L, 0)$, $(0.8L, 0)$ is used. This arrangement is the same as in Fig. 3. For all the figures in this paper, the reflection line coincides with the y -axis. The solid line represents the true (given) directional spectrum. The peak direction of the incident waves is 150° and the reflection coefficient is 1, so that the spectral peak due to the reflected waves appears at $\theta = 30^\circ$. The estimated results are shown for various values of ϵ , the ratio of the noise power to the total incident wave energy. The resolution power decreases with increasing noise component; however, the MMLM has higher resolution power than the (standard) MLM for the same amount of noise (cf. Fig. 3).

Numerical simulations were carried out for a wide range of wave gage arrangements in order to study adequate arrangements. Results were similar to the case of the standard MLM. The minimum and maximum distance between wave gages should be about $0.2L$ and $1.5L$. As can be seen from Fig. 5, the resolution power increases as the number of wave gages increases. The detailed shape of the array does not influence the result very much. This is quite different from the DFT method.

Figure 6 shows one problem in the MMLM. If the wave gages are located far from the reflection line, spurious peaks can appear in the estimated spectrum, as shown in the figure. This occurs when the modes of the standing waves at the measuring points are the same for the true and spurious peak direction. It should be possible to remove these false peaks after calculation, since they are always very sharp and recognizable. If one wave gage is located within $0.2L$ from the

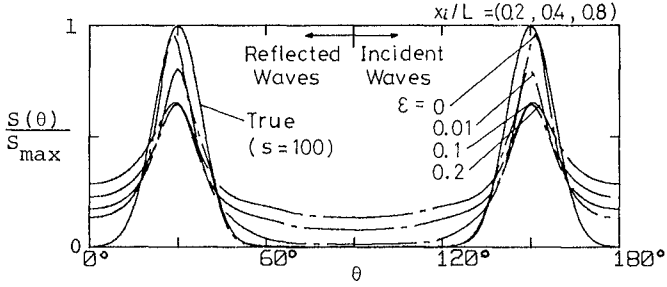


Fig. 4 Influence of noise on the resolution power of the MMLM.

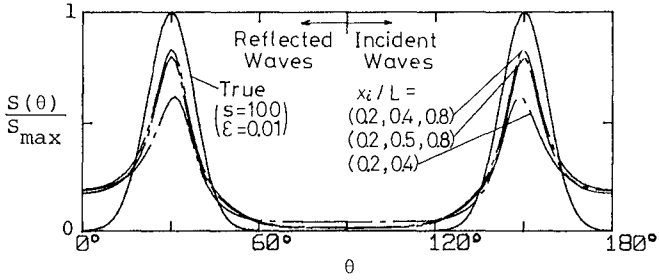


Fig. 5 Comparison among true and estimated directional spectra for various wave gage arrays.

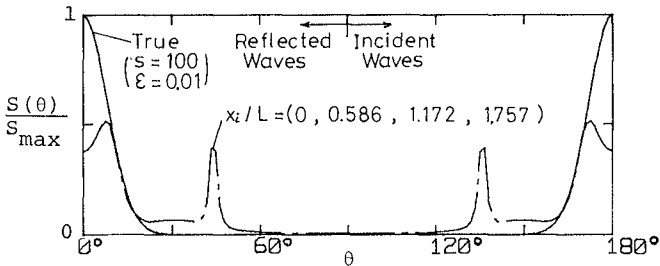


Fig. 6 Example of spurious peaks resulting from the MMLM.

reflection line and another one is about $0.2L$ from the first one, this trouble can be avoided.

From these results, linear arrays in which the distances between the reflection line and the wave gages are $0.2 l$, $0.4 l$, $0.8 l$, $1.6 l$, (l is the minimum wave length to be observed.) can be recommended. However, as will be seen later in Fig. 7(a), a 2-dimensional array is necessary to improve resolution power near the normal direction.

Figure 7 shows the results for various true directional spectra. The numbers of wave gages used are 2, 3, and 4. The array types are linear and the locations of gages are indicated in Fig. 7(a). Figure 7(a) corresponds to normal incidence. Accuracies are not high because the resolution power of the linear array in the array direction is low. A 2-dimensional array is necessary to improve resolution power in this direction. The peak incident wave direction is 120° for Fig. 7(b). Three or four-sensor arrays may have sufficient accuracy. Figure 7(c) shows the results for a uni-directional case. If the noise component is excluded, the estimated spectra should approach the true spectrum. However, since the relative noise amount of 1% was added in the numerical simulation, the resolution power for the smaller number of gages decreases significantly. Figure 7(d) corresponds to a broad spectrum. The estimated spectrum by the 4-sensor array becomes bimodal. In order to avoid this, the distance between the wave gages should be reduced. Figure 7(e) is for the bimodal incident wave spectrum. The 4-sensor array gives an accurate estimation even in this case. The reflection coefficient for Fig. 7(f) is 0.5 and the MLM is valid.

Figure 8 shows the result for a complex situation. The incident directional spectrum is bimodal and the reflection coefficient changes with direction as indicated by the solid line in the lower figure. It can be seen that many wave gages are necessary for this case.

3.3 Estimation of Reflection Coefficient

There are several possible ways to estimate the reflection coefficient. Equation (37) gives an estimation of the reflection coefficient at the peak direction, θ_m . This can be defined as a representative reflection coefficient, denoted by r_m :

$$r_m = r(\theta_m) \quad (40)$$

A second definition is as the square root of the ratio between the reflected and incident spectra estimated at the peak direction:

$$r_{sm} = \sqrt{\hat{S}(\theta_{mr}) / \hat{S}(\theta_m)} \quad (41)$$

where θ_{mr} is the reflected wave direction corresponding to the incident peak direction. A third definition is as the square root of the ratio between the integrated reflected and incident wave energy:

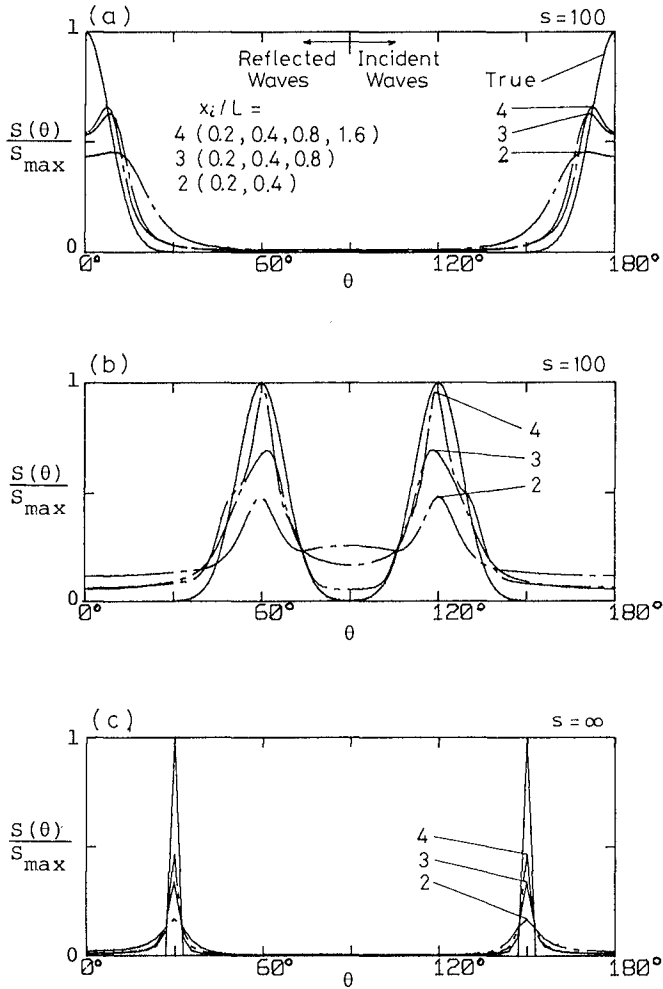


Fig. 7 Comparison among true and estimated directional spectra for various true spectra. (continued)

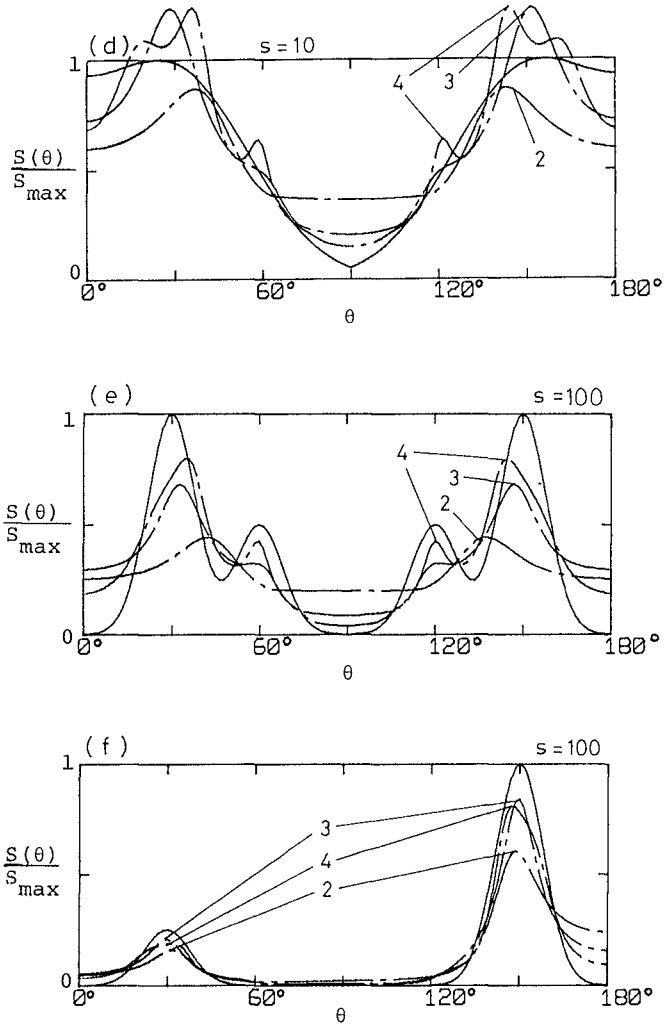


Fig. 7 Comparison among true and estimated directional spectra for various true spectra.

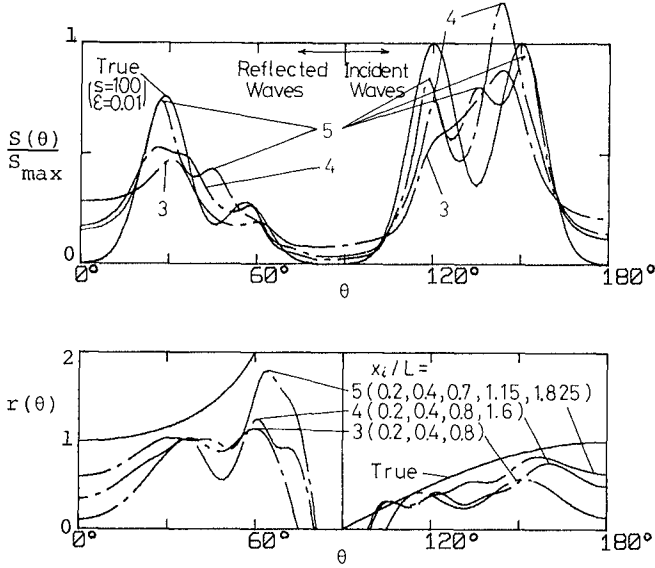


Fig. 8 Comparison among true and estimated directional spectra and reflection coefficients for a complex wave field.

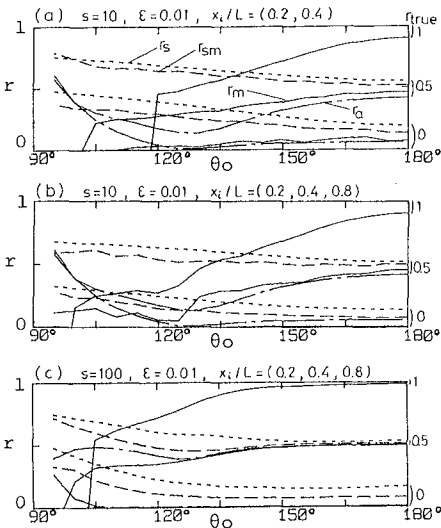


Fig. 9 Comparison among true and estimated reflection coefficients.

$$r_s = \sqrt{\frac{\int_{\text{ref.}} \hat{S}(\theta) d\theta}{\int_{\text{in.}} \hat{S}(\theta) d\theta}} \quad (42)$$

For the uni-directional case, the reflection coefficient can be calculated from data records at two points (Goda and Suzuki, 1976, for example). When the two points are on the x-axis, this can be written by using the results of a spectral analysis as

$$r_a = \sqrt{\frac{1 + c^2 - 2c \cos(kd \cos\theta_0 - \Delta)}{1 + c^2 + 2c \cos(kd \cos\theta_0 - \Delta)}} \quad (43)$$

where c is the ratio of the power spectra, Δ is the phase lag, and d is the distance between the measuring points.

Figure 9 compares the true and estimated reflection coefficients. The Mitsuyasu-type directional distributions were used with $s = 10$ for Fig. 9(a) and (b) and $s = 100$ for Fig. 9(c). For true reflection coefficients of 0, 0.5 and 1, the estimated values are plotted against the peak incident wave direction. The solid, dashed, dotted, and chain lines indicate the values of r_m , r_{sm} , r_s and r_a , respectively. As seen from Fig. 9(a), a 2-sensor array may not be sufficient. If a 3-sensor array is used, r_m gives a fairly accurate value when the true reflection coefficient is small, whereas r_{sm} is relatively accurate for large values. However, the error is large when the peak incident direction is nearly parallel to the reflection line.

4. CONCLUSION

In an incident and reflected wave field, extra terms which may be called phase interaction terms, appear in the relationship between the directional spectrum and the cross-power spectrum. If the wave gage array is located near the reflection line, this contribution becomes significant and therefore the standard MLM is not applicable. The MLM was modified for estimating the directional spectrum in such a situation and the method was named the MMLM (Modified Maximum Likelihood Method). The final result is expressed by Eq. (38).

Numerical simulations were carried out to examine the validity of the MMLM. The results demonstrated that the MMLM has high resolution power and can separate incident and reflected wave energies. The resolution power increases with increasing number of wave gages, but the effect of the detailed wave gage arrangement is small. In general, the minimum and maximum distance between the wave gages should be about $0.2L$ and $1.5L$. However, these criteria depend upon the number of gages and the width of the directional distribution. Spurious spectral peaks appear if the wave gages are located far from the reflection line. If the wave gages are located at $0.2l$, $0.4l$, $0.8l$, $1.6l$, ... (l is the minimum wave length to be observed) from the reflection line, the array is effective for wide range of wave length. A 2-dimensional array is necessary to improve the resolution power near the direction normal to the reflection line.

Various formulas to estimate the reflection coefficient were examined. As long as the peak incident wave direction is not coincident with the reflection line, the reflection coefficient, r_m , determined directly by the MMLM is accurate for small values of the true reflection coefficient, whereas the reflection coefficient determined from the resulting power ratio of the incident and reflected waves, r_{sm} , is accurate for large values.

REFERENCES

- 1) Barber, N.F. (1963): The directional resolving power of an array of wave detectors, *Ocean Wave Spectra*, Prentice-Hall, Inc., New Jersey, pp. 137-150.
- 2) Capon, J. (1969): High-resolution frequency-wavenumber spectrum analysis, *Proc. IEEE*, Vol. 57, No. 8, pp. 1408-1418.
- 3) Davis, R.E. and L.A. Regier (1977): Methods for estimating directional wave spectra from multi-element arrays, *J. Mar. Res.*, Vol. 35, No. 3, pp. 453-477.
- 4) Goda, Y. and Suzuki, Y. (1976): Estimation of incident and reflected waves in random wave experiments, *Proc. 15th Coastal Eng. Conf.*, ASCE, pp. 828-845.
- 5) Isobe, M., K. Kondo and K. Horikawa (1984): Extension of MLM for estimating directional wave spectrum, *Proc. Symp. on Description and Modelling of Directional Seas*, Copenhagen, pp. A-6-1 - A-6-15.
- 6) Koopmans, L.H. (1974): *The Spectral Analysis of Time Series*, Academic Press, New York, 366p.
- 7) Longuet-Higgins, M.S., D.E. Cartwright and N.D. Smith (1963): Observations of the directional spectrum of sea waves using the motions of a floating buoy, *Ocean Wave Spectra*, Prentice Hall, Inc., New Jersey, pp. 111-136.
- 8) Mitsuyasu, H., F. Tasai, T. Subara, S. Mizuno, M. Okusu, T. Honda and K. Rikiishi (1975): Observation of the directional spectrum of ocean waves using a clover-leaf buoy, *J. Phys. Oceanogr.*, Vol. 5, pp. 750-760.
- 9) Oltman-shay, J. and R.T. Guza (1984): A data adaptive ocean wave directional spectrum estimator for pitch and roll type measurements, *J. Phys. Oceanogr.* (in press)
- 10) Panicker, N.N. and L. E. Borgman (1974): Enhancement of directional wave spectrum estimates, *Proc. 14th Coastal Eng. Conf.*, ASCE, pp. 258-279.